Bounding the success probability of naval mine-clearance missions conducted by AUVs

D. Esnault[1,2], S. Rohou[2], F. Le Bars[2], and L. Jaulin[2]

[1]DGA Naval Systems, Brest, France
[2]ROBEX Team, Lab-STICC, ENSTA, Brest, France

June 19, 2025

Abstract

The success of mine-clearance missions conducted by Autonomous Underwater Vehicles (AUVs) mainly depends on two inter-related factors: the AUV behavior and the validation of a mission assumption. AUVs are typically modeled as stochastic dynamical systems and controlled using probabilistic techniques, such as Kalman filtering, to handle environmental uncertainties and inherent behavioral randomness. Assumption validation, on the other hand, often relies on set-based conditions, such as detecting an object on the seabed using an onboard exteroceptor, resulting in a three-valued logic outcome: success, failure, or uncertain. Thus, estimating mission success involves computing the probability of an event whose realization can be uncertain and influenced by a stochastic system (i.e. the AUV). In this paper, we extend traditional binary outcome models to a three-valued logic framework and introduce an empirical estimator based on the Monte Carlo method to bound the success probability within an interval. As with the standard binary outcome Monte Carlo estimator, the accuracy of this estimated interval improves with the number of trials, following the law of large numbers.

Keywords

Probabilities, Interval methods, Empirical estimators, Underwater robotics

1 Introduction

Autonomous Underwater Vehicles (AUVs) are gradually transforming how we perceive, explore and interact with the underwater environment. Over the past few decades, these ground-breaking vehicles have evolved from experimental prototypes to precise and reliable systems, capable of operating in challenging conditions without human intervention. They are used in various applications, such as ocean exploration [1] [2], coastal mapping [3] [4] and even underwater infrastructure inspection [5] [6]. The defense sector is also increasingly using AUVs for missions like the surveillance of strategic areas (e.g. ports or transit zones) [7] or the reconnaissance of objectives in hostile environments (e.g. preparations for landings) [8].

Among these applications, one stands out more than the others: mine-clearance. The goal of a mine-clearance operation is to secure a maritime area (e.g. a port or a navigation corridor) by locating and neutralizing all dangerous objects, such as naval mines. Traditionally, mine-clearance operations have been conducted by dedicated vessels crewed with trained and specialized navy personnel. However, with the development of AUVs, it is now possible to keep man away from the threat, replacing crewed vessels by unmanned naval vehicles [9]. While humans are still involved in the decision-making process, particularly in analyzing data and making critical judgments, they can now operate remotely, beyond the reach of danger.

There are several types of naval mine (see Figure 1), ranging from drifting surface mines to buried mines. For simplicity, we will only focus on bottom mines (i.e. mines lying on the seabed) but our results could be easily extended to other cases. A bottom mine can be characterized as a remarkable, unnatural and dangerous object standing on the seabed. To find and neutralize these threats, a mine-clearance mission generally progresses in four stages:

1. Detection: Detect all remarkable objects lying on the seabed within the area.
2. Classification: Categorize detected objects as either natural or non-natural.
3. Identification: Assess whether the non-natural classified objects are dangerous.
4. Neutralization: Detonate objects identified as dangerous.

Due to their low-risk nature, the first two stages can be carried out using AUVs equipped with high-performance navigation payloads and advanced perception sensors. This configuration offers high coverage rate and reliable detection capabilities. However, despite the quality of their navigation payloads, AUVs are generally subject to position drift due to the uncertainty accumulated during navigation [11]. This results in approximate positioning of seabed objects, with accuracy depending on when the AUV detects the objects during the mission.

On the other hand, due to their dangerous nature, the last two stages can only be carried out by AUVs equipped with low-grade navigation payloads and basic perception sensors. This configuration results in a low-cost and potentially expendable vehicle. However, the use of low-precision navigation payloads leads to high positioning uncertainty during navigation and, consequently, potentially unpredictable AUV behavior.

Consequently, a mine-clearance mission conducted with AUVs typically involves two different types of vehicles and is carried out in two successive phases. The first phase is performed by a high-performance and expensive AUV tasked with detecting, classifying, and locating non-natural objects on the seabed. The second phase involves low-cost and expendable AUVs that are deployed to relocate the previously detected objects in order to identify and potentially neutralize them. The second phase poses a major technical challenge, requiring the relocation of objects with only approximate positions using low-cost AUVs that may behave unpredictably. These uncertainties raise serious concerns about the reliability and overall feasibility of identification and neutralization operations conducted by AUVs.

The identification stage being critical, as it determines whether an object is a mine or not, failure in finding the object, or worse, identifying the wrong object, can lead to serious consequences, including the loss of human life. To make informed decisions (i.e. whether to carry out the identification using AUVs or human divers), the operator in charge of mission planning must therefore know the feasibility of the mission or, at least, have an estimate of it. The aim of this paper is to provide this same operator with a reliable and understandable indicator for decision-making.

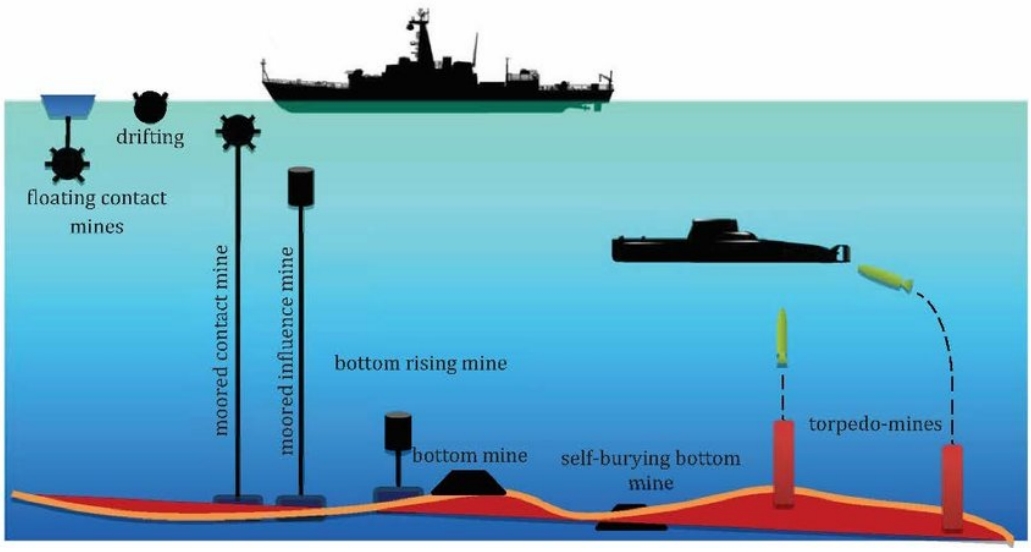


Figure 1: Classification of various types of naval mines.
(Extracted from [10])

The most straightforward indicator to interpret is the probability of mission success. In other words, this is the likelihood that the AUV used for identification will successfully relocate the object to be identified. To calculate this probability of success, we will first model the problem to define what represents a successful outcome, identify the parameters that affect whether this outcome is achieved and determine a method to reliably and precisely compute the success probability.

2 Problem modeling

The success of an identification mission conducted by an AUV, and more broadly, the success of any underwater mission performed by an AUV, hinges on two critical factors:

- The AUV's behavior during the mission.
- The validation of a key assumption.

For example, consider the following scenario: at the end of the detection and classification stages, a non-natural object, which could potentially be a bottom mine, has been detected, classified, and located. To determine the nature of this suspicious object, an AUV is deployed for an identification mission. The identification AUV is equipped with a low-cost inertial navigation system (INS) and with a waterproof camera. Its task is to reach the estimated position of the object and acquire visual data through its integrated camera system. To validate the mission, a key assumption must be satisfied: the camera must successfully capture images of the suspect object. Since the camera is mounted on the AUV, meeting this condition is directly linked to the trajectory followed by the vehicle (i.e. its behavior). We can therefore conclude that the success of an identification mission conducted by an AUV corresponds to the validation of a key assumption that is dependent on the AUV's behavior. Having defined what constitutes a successful outcome (i.e. the validation of a key assumption) and identified the parameters that affect whether this outcome is achieved (i.e. the AUV's behavior), the next step is to model them to develop a method for calculating the probability of success.

Autonomous Underwater Vehicles (AUVs) are complex dynamical systems that integrate various sensors, actuators, and algorithms to autonomously accomplish their missions. These vehicles also operate in vast, dynamic, and often unknown environments, necessitating continuous adaptation of their behavior [13]. As a result, the behavior of an AUV is shaped by a variety of influencing factors that may be uncertain (e.g. sensor measurements), dynamic (e.g. ocean currents) or random (e.g acoustic communication loss), all of which must be accounted for to ensure reliable and adaptive operation in real-world conditions.

To account for various sources of uncertainty, AUVs are typically modeled as stochastic dynamical systems, with control strategies based on probabilistic assumptions. For instance, sensor noise is often modeled as Gaussian [14], which represents the random errors typically found in sensor measurements. Filtering techniques, such as the Kalman filter [15], are commonly used to process this noisy data, allowing for more accurate estimation of the AUV's true state by reducing the effect of these errors. In summary, the behavior of an AUV is inherently stochastic. Even when operating under similar environmental conditions and with identical mission plans, the AUV's trajectory will vary.

In this paper, we will therefore model the identification AUV as a random system S. A realization R_S of the system S corresponds to a possible trajectory described by the AUV for a same mission and environment. A trajectory is defined as a function from $\mathbb{R}$ to $\mathbb{R}^n$, mapping each instant $t \in \mathbb{R}$ to a possible state $\mathbf{X} \in \mathbb{R}^n$ of the robot. The set of all realizations of the system is denoted $\{R_{S,i}\}_{i=1}^{N}$, where $R_{S,i}$ corresponds to the i-th realization of S and $N \in \mathbb{N}^*$ represents the total number of realizations performed or simulated. As explained earlier, the aim of an identification mission is to relocate a suspect object in order to acquire more information about it, and determine its nature. The key assumption to validate is whether the object was seen by the AUV during the mission. If so, the mission is considered a success; if not, it's a failure.

For the sake of simplicity, the object is generally considered to be punctual, i.e. it is represented by a point (often its center) and it is assumed that seeing this point is sufficient to identify the object's nature. This assumption is coherent in terms of scale (i.e. the size of a mine compared to the size of the search area and the perception capacity of the sensors), but it must be nuanced by recalling that the object is uncertainly positioned. In fact, as detailed above, the AUV in charge of detecting and locating objects accumulates navigational uncertainty as the mission progresses, which leads to uncertainty in the object's positioning. In reality, to maximize the chances of seeing the object, the aim is not simply to cover the point, but to cover an area centered on the point, the size of which will depend on the uncertainty of the object's position. For example, if the object is positioned with an estimated uncertainty of ± 5 meters, a circular zone centered on the object's estimated position, and with a radius of at least 5 meters, will have to be covered to compensate for the positioning uncertainty. Consequently, we can model the object to be found as a punctual object contained in a set $\mathbb{O}$ (i.e. the search zone), which the AUV will have to cover with its sensors to succeed in its mission.

To identify the object, the AUV is equipped with one or more perception sensors. Each sensor has its own perception capabilities. For example, in two dimensions, the perception zone of a camera or frontal sonar is generally modeled by a cone whose position and orientation depend on the position and orientation of the robot. As the AUV moves along its trajectory, the perception sensors will progressively cover an area of the seabed, which we will refer to as set $\mathbb{C}$. If a point is in set $\mathbb{C}$, then there is at least one instant in the mission where this point will have been seen by the AUV; conversely, if the point is not in set $\mathbb{C}$, then there is no instant in the mission where the point has been seen by the AUV.

Therefore, to find out whether the AUV has seen the object during its mission, it is only a question of verifying whether set $\mathbb{O}$ is included in set $\mathbb{C}$. At the end of the mission, three realizations are then possible (as illustrated in Figure 2):

1. Set $\mathbb{O}$ and set $\mathbb{C}$ are disjoint ($\mathbb{O} \cap \mathbb{C} = \varnothing$): None of the object's possible positions are covered by the sensor, so the AUV will not be able to see the object, whatever its position. In this case, mission failure is guaranteed.

2. Set $\mathbb{O}$ is partially in set $\mathbb{C}$: Part of the object's possible positions are covered by the sensor, and the rest are not. No conclusion can be drawn, depending on its position in $\mathbb{O}$, the object may or may not be seen. The success of the mission is therefore uncertain.

3. Set $\mathbb{O}$ is entirely within set $\mathbb{C}$ ($\mathbb{O} \subseteq \mathbb{C}$): All possible positions of the object are covered by the sensor, so the AUV will be able to see the object, whatever its position in set $\mathbb{O}$. In this case, mission success is guaranteed.

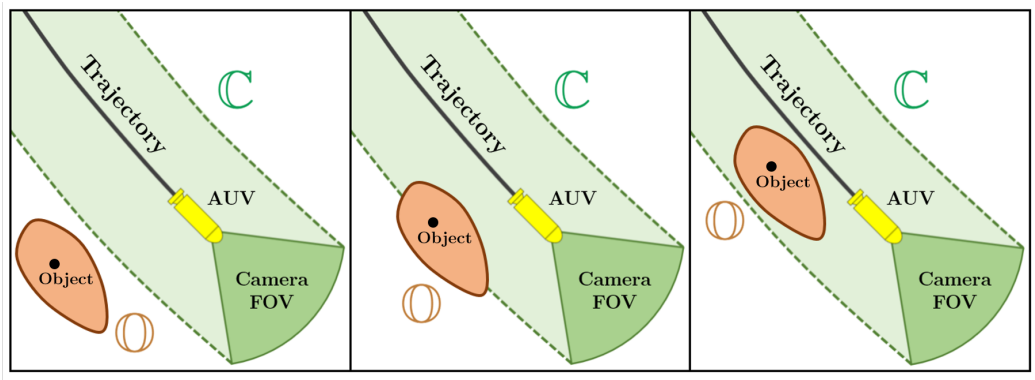


Figure 2: Illustration of the possible outcomes for an identification mission conducted by a camera-equipped AUV.

(Left) Mission failure is guaranteed.
(Middle) Mission success is uncertain.
(Right) Mission success is guaranteed.

By modeling the object and the area covered by the sensors as sets, the key assumption therefore doesn't follow a standard binary realization (success or failure), but rather a three-value logic (success, failure or uncertain) [16]. To summarize, determining the probability of success of an identification mission carried out by an AUV is equivalent to calculating the probability of occurrence of an event E (i.e. the key assumption) whose realization is uncertain (i.e. follows a three valued-logic) and is dependent on a random system S (i.e. the AUV). The quantity we wish to calculate is therefore $P_{E(S)}$, which we shall refer to as P_E in the following for the sake of clarity.

3 Monte-Carlo method

Estimating the probability of success P_E for an AUV identification mission is challenging due to the system's inherent complexity and the numerous sources of uncertainty involved. One possible approach is to develop a fully analytical model of the system and derive an exact expression for P_E. While attractive in theory, this method quickly becomes impractical in real-world scenarios, as it requires modeling a high-dimensional space of variables with nontrivial interactions.

A more feasible alternative is to approximate P_E using an estimator. As with the choice of the feasibility indicator, the estimator must be simple, accessible, and robust enough to support decision-making by non-specialist operators. In this context, we adopt an estimator based on the Monte Carlo method [17]. The Monte Carlo method is an empirical approach that estimates the probability of an event E' by simulating a large number of independent trials. For each trial, system behavior is sampled under varying input conditions and uncertainties, and the occurrence of the event is recorded. In the case of binary outcomes (success or failure), the probability of success is approximated by the proportion of successful trials:

$$P_{E'} \approx \frac{1}{N'} \sum_{i=1}^{N'} \delta_{E'}(x_i) \tag{1}$$

where $N' \in \mathbb{N}^*$ is the total number of trials, x_i denotes the i-th simulated trial, and $\delta_{E'}(x_i)$ is an indicator function equal to 1 if the event E' occurs in the trial x_i, and 0 otherwise [18]. This estimator is unbiased, and its accuracy improves with the number of trials, as guaranteed by the law of large numbers [19].

In the context of an identification mission carried out by an AUV, the trials $\{x_i\}_{i=1}^N$ represent the trajectories $\{R_{S,i}\}_{i=1}^N$ that could be described by the AUV during a given scenario. Since the objective is to estimate the probability of success P_E before the mission and within a reasonable period of time, it is not feasible to physically send the AUV to repeat the same mission several times in order to obtain the empirical samples $\{R_{S,i}\}_{i=1}^N$. This approach would be costly, time-consuming and unrealistic.

One relevant approach is to use a high-fidelity simulator to reproduce the AUV's behavior numerically. By running a sufficient number of simulations of the same mission, varying, for example, random parameters linked to navigation uncertainties, currents or sensor disturbances, it is possible to generate a set of representative virtual trajectories $\{R_{S,i}\}_{i=1}^{N}$. These simulated trajectories are then used as samples to estimate the probability of mission success P_E. Consequently, the Monte Carlo estimator $\hat{P_E}$ for an identification mission conducted by an AUV can be formulated as follows:

$$\hat{P_E} = \frac{1}{N} \sum_{i=1}^{N} \delta_E(R_{S,i}) \tag{2}$$

where $N \in \mathbb{N}^*$ is the total number of simulated trajectories, $R_{S,i}$ represents the i-th simulated trajectory and $\delta_E(\cdot)$ is the indicator function for the event E.

A key difficulty arises in defining the indicator function for the event E when its outcome is not strictly binary. In the standard Monte Carlo method, the event E' is associated with a binary outcome (success or failure), allowing a straightforward definition of the indicator function $\delta_{E'}(\cdot)$, which takes the value 1 if E' occurs in a given trial, and 0 otherwise. In contrast, the event E may result in an uncertain realization, introducing ambiguity in the indicator function's definition. While it remains trivial to assign a value of 1 when E clearly occurs and 0 when it clearly does not, the uncertain case introduces a challenge, as the occurrence of E cannot be definitively confirmed or rejected. To apply the Monte Carlo estimator in the presence of uncertain outcomes, it is necessary to introduce a method that accounts for this ambiguity, which could arises frequently during simulations.

4 Interval analysis

To handle uncertainty in the evaluation of the indicator function associated with event E, several modeling strategies can be considered.

A first, naive approach would be to treat all uncertain realizations as failures by assigning them a value of 0 in the indicator function $\delta_E(\cdot)$. In this case, uncertainty about the occurrence of E is translated into pessimism in the estimation of P_E, resulting in a loss of potentially useful information for the operator. Consider, for example, an identification mission where the AUV follows trajectories and, for each one, is able to cover 99% of the search area $\mathbb{O}$. Although object detection is not strictly guaranteed, the probability of success is irrefutably high. Nevertheless, under this pessimistic model, the indicator would treat every such trajectory as a failure, yielding an estimated success probability of zero. This significant information loss makes the approach undesirable in practical settings.

An alternative idea is to allow the indicator function to return a value between 0 and 1 in cases where the realization of E is uncertain. This would enable the quantification of the "degree of belief" or "level of uncertainty" associated with each realization and allows it to influence the estimate of P_E. In the example above, one might assign a value of 0.99 to each trajectory based on the 99% coverage of $\mathbb{O}$, resulting in an overall estimate of $\hat{P_E} = 0.99$. While appealing, this approach raises a fundamental issue.

The main drawback is that the choice of the value to assign to an uncertain realization becomes inherently subjective. One operator might base the assignment solely on coverage, while another might incorporate mission duration, battery level, or additional contextual factors. This leads to multiple, equally plausible estimates of P_E for the same underlying data, making the final decision dependent on subjective criteria. Consequently, the indicator function loses its objective interpretability.

To model the uncertainty in the realization of E more rigorously, we propose to use *interval analysis*. Initially introduced to rigorously bound errors in numerical computations [20], interval analysis has since been extended to various applications in engineering and robotics, including state estimation and robust control [21]. It provides a reliable mathematical framework for handling uncertainty in a guaranteed and systematic way.

An *interval* $[x]$ is defined as a closed, connected subset of $\mathbb{R}$, bounded by a lower limit x^- and an upper limit x^+ [20]:

$$[x] = [x^-, x^+] = \{x \in \mathbb{R} \mid x^- \leq x \leq x^+\} \tag{3}$$

The set of all real intervals is denoted $\mathbb{IR}$. The *width* of an interval is defined as $w([x]) = x^+ - x^-$. When $x^- = x^+$, the interval is said to be *degenerate* and represents a single real number.

Interval arithmetic extends conventional operations to intervals. Given two intervals $[x], [y] \in \mathbb{IR}$ and a binary operator $\star \in \{+, -, \cdot, /\}$, the operation $[x] \star [y]$ is defined as the smallest interval that contains all possible outcomes of $x \star y$, for $x \in [x]$ and $y \in [y]$:

$$[x] \star [y] = [\{x \star y \mid x \in [x],\ y \in [y]\}] \tag{4}$$

Here, $[\{\cdot\}]$ denotes the *convex hull*, i.e., the smallest interval containing the set.

In practice, many operations on intervals can be computed directly on the bounds. For example, adding two intervals $[x]$ and $[y]$ or multiplying an interval $[x]$ with a real value $\lambda \in \mathbb{R}$:

$$[x] + [y] = [x^- + y^-,\ x^+ + y^+] \tag{5}$$

$$\lambda \cdot [x] = \begin{cases} [\lambda x^-,\ \lambda x^+] & \text{if } \lambda \geq 0 \\ [\lambda x^+,\ \lambda x^-] & \text{if } \lambda < 0 \end{cases} \tag{6}$$

To adapt the Monte Carlo method to a three-valued logic framework, we propose quantifying uncertain realizations of event E using the interval $[0, 1]$. This interval reflects the fact that, in such cases, success or failure cannot be definitively determined. In contrast, realizations that are known to be successful or failed are represented by degenerate intervals [1] and [0], respectively. Thanks to interval arithmetic, it is also possible to perform operations on intervals, such as computing the mean of all the intervals returned by the indicator function.

5 Three-valued logic Monte-Carlo method

By applying the Monte Carlo method with the interval-valued indicator function, the output is no longer a scalar estimate but rather an interval $[P_E]$, obtained by averaging the interval evaluations of the indicator function $[\delta_E](\cdot)$ over N simulated trajectories:

$$[P_E] = \frac{1}{N} \sum_{i=1}^{N} [\delta_E](R_{S,i}) \tag{7}$$

where $N \in \mathbb{N}^*$ is the number of simulations, $R_{S,i}$ denotes the i-th simulated trajectory, and the interval-valued indicator function $[\delta_E](\cdot)$ is defined as:

$$[\delta_E](R_{S,i}) = \begin{cases} [1] & \text{if success is guaranteed,} \\ [0] & \text{if failure is guaranteed,} \\ [0, 1] & \text{if the outcome is uncertain.} \end{cases} \tag{8}$$

In contrast to the standard binary-outcome Monte Carlo method, which produces a scalar estimate $\hat{P_E}$ that converges to the true probability P_E as the number of simulations increases, the interval-based approach yields an interval $[P_E]$. This interval serves as a bound, but does not inherently guarantee that it contains the true value of P_E. Rather, it is the law of large numbers that ensures that, as the number of simulations grows, the interval $[P_E]$ becomes increasingly narrow and reliable, thereby improving the likelihood that it encloses the true success probability P_E.

The three-valued logic-adapted Monte Carlo method, which constitutes the core contribution of this work, enables the computation of a mission success bound $[P_E]$. When used as a feasibility indicator for AUV identification missions, this bound provides operators with a reliable basis for decision-making under uncertainty.

6 Application

To illustrate our approach, let's consider the following scenario: during a mine-clearance mission, three unnatural objects have been detected, classified and located on the seabed. An identification mission must then be planned to determine the exact nature of these objects. To this end, an AUV (Autonomous Underwater Vehicle) would be deployed. The AUV is equipped with a waterproof camera, fixed to the underside of the AUV and pointing downwards, to capture images of the seabed during the mission (see Figure 3).

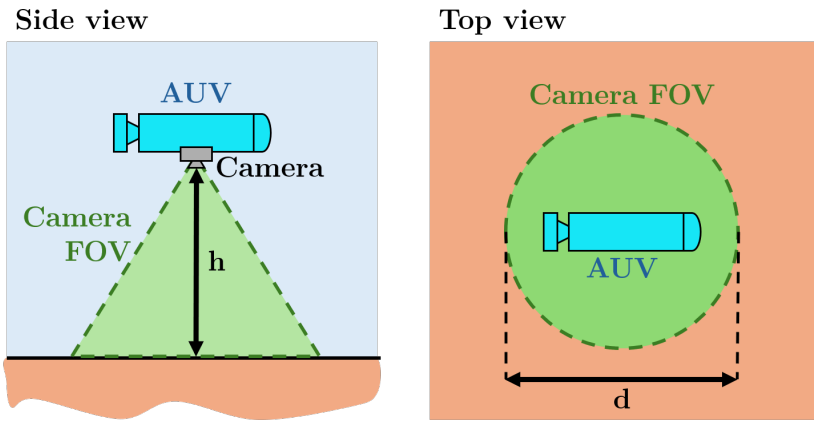


Figure 3: Illustration of AUV camera configuration.
(Left) Side view of the AUV. (Right) Top view of the AUV.

At a given moment, the area of the seabed covered by the camera can therefore be modeled by a disk of diameter d, which is a function of the camera's aperture angle and the AUV's altitude h relative to the seabed. For simplicity's sake, we'll assume that the AUV evolves at a constant altitude, thus reducing the problem to a two-dimensional space.

The suspect objects to be identified have been located in an uncertain manner. To model these uncertainties, each object is assigned a search zone, represented by a rectangular box (or *bounding box*). Each box is assumed to contain one object whose exact position within the box remains unknown. The identification mission consists, for the AUV, in following a trajectory predefined by a human operator, while continuously acquiring images using its camera (see Figure 4). The mission is considered a success if, during this trajectory, the AUV manages to cover all three search zones, thus ensuring the acquisition of images of all three suspect objects.

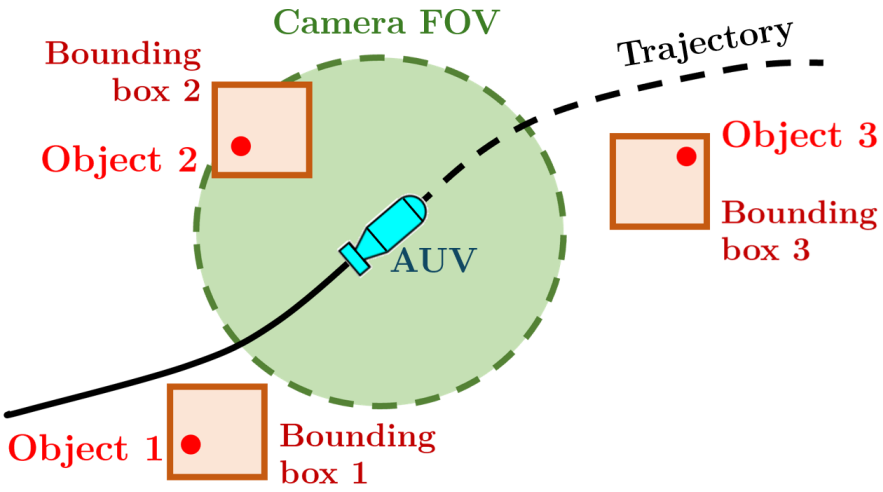


Figure 4: Illustration of the mission scenario.

For the sake of simplicity, the dynamic of the AUV is modeled as a Dubins car moving on the plane at constant speed $v(t) = 1$ m/s [23]:

$$\dot{\mathbf{X}}(t) = \mathbf{f}(\mathbf{X}(t), u_\theta(t)) = \begin{pmatrix} \cos(\theta(t)) \\ \sin(\theta(t)) \\ u_\theta(t) \end{pmatrix} \tag{9}$$

where $\mathbf{X}(t) = (x(t), y(t), \theta(t))^\top$ is the state vector of the AUV, and $u_\theta(t)$ is the control input for the heading. The state vector $\mathbf{X}$ consists of the position coordinates x and y of the AUV in the horizontal plane, and θ, its heading angle. It will be assumed that the initial state vector $\mathbf{X}_0 = \mathbf{X}(t_0)$ of the AUV is perfectly known.

To introduce randomness into the AUV's behavior, we assume that the command $u_\theta(\cdot)$ is affected by additive white Gaussian noise $\beta \sim \mathcal{N}(0, \sigma^2)$. Thus, the command applied to the AUV becomes $u_\theta(t) + \beta(t)$. Using a numerical integration method such as the Euler scheme [24], the behavior of the AUV can be simulated over the time interval $[t_0, t_f] \in \mathbb{IR}$, with a numerical integration time step $dt \in \mathbb{R}_+^*$, using the following evolution equation:

$$\mathbf{X}(t + dt) = \mathbf{X}(t) + dt \cdot \dot{\mathbf{X}}(t) \tag{10}$$

$$= \begin{pmatrix} x(t) + dt \cdot \cos(\theta(t)) \\ y(t) + dt \cdot \sin(\theta(t)) \\ \theta(t) + dt \cdot (u_\theta(t) + \beta(t)) \end{pmatrix} \tag{11}$$

To generate a set of trajectories $\{R_{S,i}\}_{i=1}^N$ using this scheme, we only need to initialize the AUV to the $\mathbf{X}_0$ state and simulate its evolution using the evolution equation. This process is repeated N times to generate the desired number of trajectories (see Figure 5). In our specific case, since the area covered by the camera at a given time is a disk centered on the AUV's rotation center, the observed area remains invariant to the AUV's orientation. As a result, a trajectory $R_{S,i}$ is defined as a function from $\mathbb{R}$ to $\mathbb{R}^2$, mapping each instant $t \in [t_0, t_f]$ to a possible position $(x(t), y(t))^\top$ of the robot.

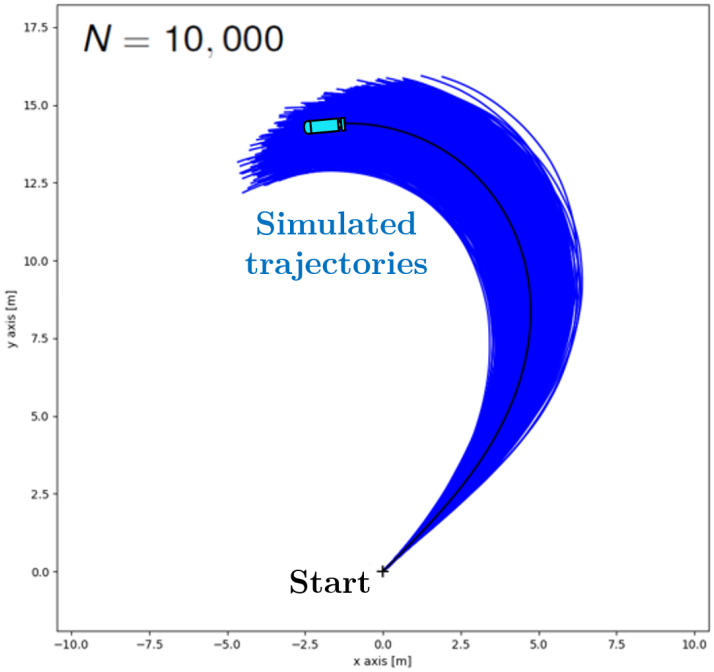


Figure 5: Display of the 10,000 simulated AUV trajectories.

Once the trajectories $\{R_{S,i}\}_{i=1}^{N}$ have been generated, we need to evaluate the realization of the mission for each of them, i.e. determine the value returned by the indicator function $[\delta_E](\cdot)$ for each trajectory $R_{S,i}$. In this scenario, the event E to be validated corresponds to complete coverage of the three bounding boxes associated with the suspect objects during a single trajectory. For each trajectory $R_{S,i}$, three outcomes can therefore occur:

1. Guaranteed success ($[\delta_E](R_{S,i}) = [1]$): all three bounding boxes are completely covered over the trajectory (see Figure 6).
2. Guaranteed failure ($[\delta_E](R_{S,i}) = [0]$): at least one bounding box is not covered at all. This means that at least one object cannot be detected, and the mission is considered to have failed (see Figure 7).
3. Uncertain success ($[\delta_E](R_{S,i}) = [0, 1]$): at least one bounding box is partially covered, without any being completely missed. This means that at least one object detection is uncertain (see Figure 8).

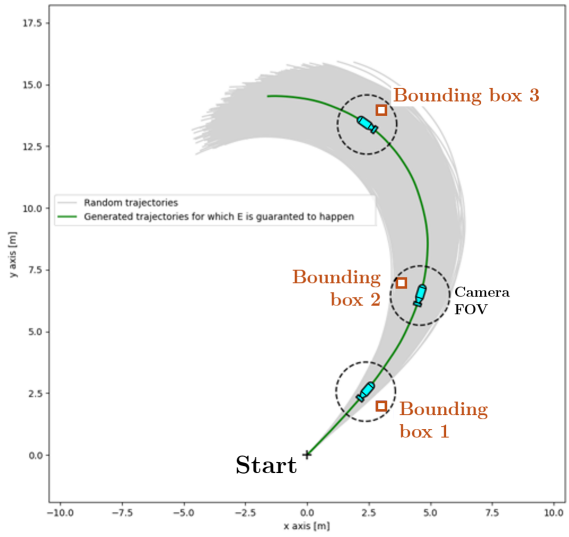


Figure 6: Display of one of the simulated trajectories where mission success is guaranteed (in green).

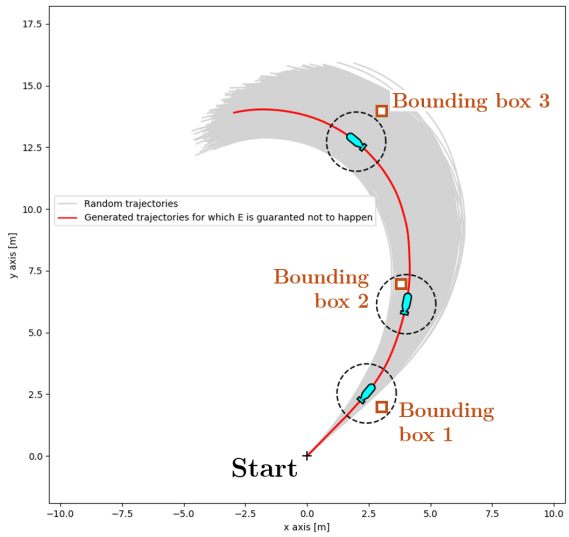


Figure 7: Display of one of the simulated trajectories where mission failure is guaranteed (in red).

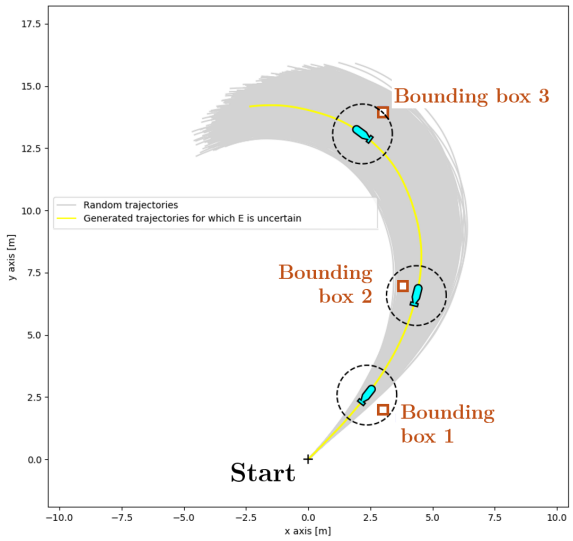


Figure 8: Display of one of the simulated trajectories where mission success is uncertain (in yellow).

Finally, we evaluate the indicator function $[\delta_E](\cdot)$ over each trajectory in $\{R_{S,i}\}_{i=1}^{N}$ (see Figure 9). By averaging the resulting intervals as defined in (7), we compute the probability interval $[P_E]$, which will serve as a feasibility indicator for the operator in charge of mission planning.

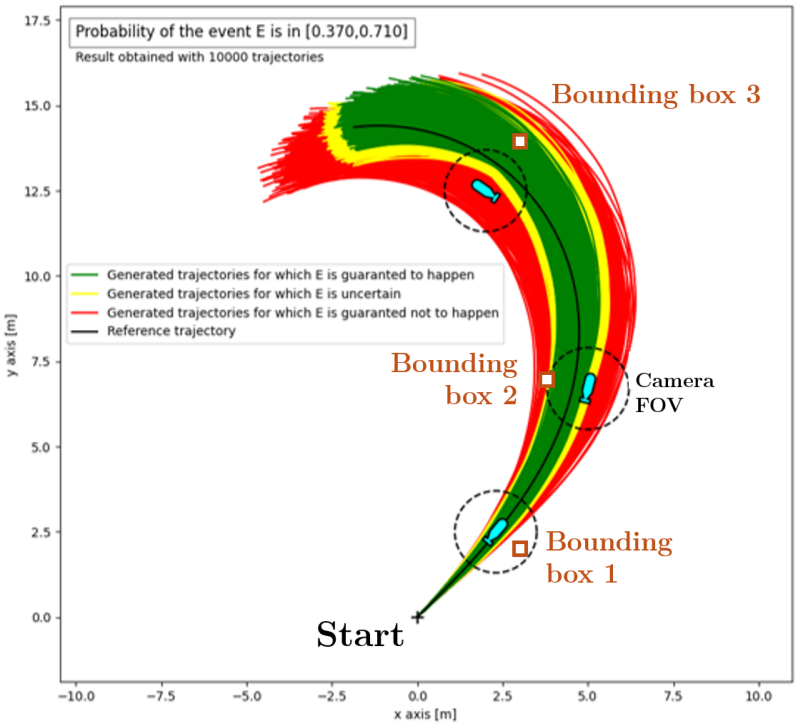


Figure 9: Display of all the simulated trajectories and their evaluations in the realization of the event E.

As detailed above and in accordance with the law of large numbers, Figure 10 shows that, as the number of samples increases, the interval $[P_E]$ converges to a stabilized interval, assumed to contain the true probability of success P_E.

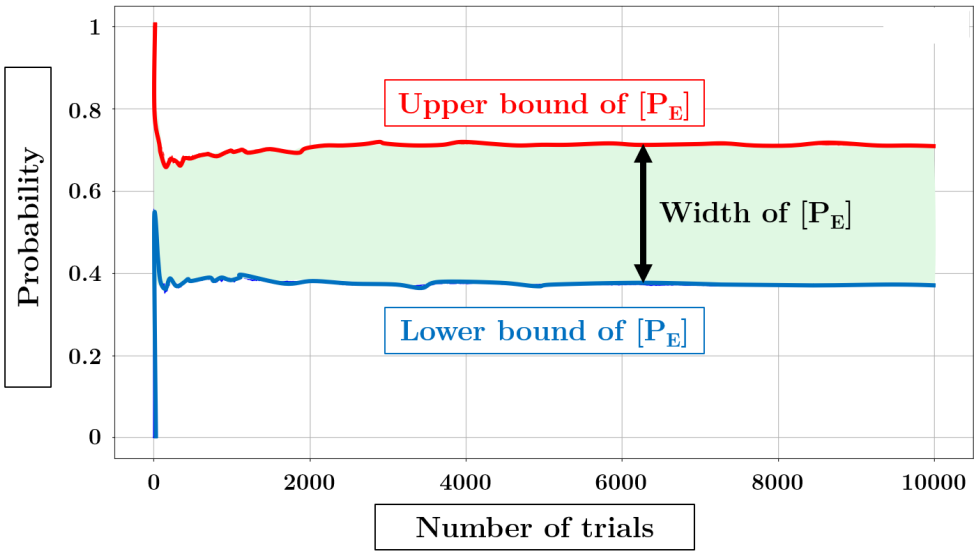


Figure 10: Evolution of the width of the interval $[P_E]$ as a function of the number of trajectories evaluated.

7 Conclusion

This paper addressed a critical challenge in naval mine-clearance: evaluating the feasibility of AUV-based identification missions under uncertainty. Standard binary-outcome models fall short in operational environments where partial sensor coverage and uncertain object positioning are the norm. To bridge this gap, we introduced a novel three-valued logic framework coupled with an interval-based Monte Carlo method.

Unlike traditional estimators, our approach captures the inherent ambiguity of real-world missions by bounding the success probability within an interpretable interval. This bound provides a more honest, transparent metric for mission planning—especially in high-stakes defense scenarios where overconfidence can lead to severe consequences.

Beyond its immediate utility in single-AUV planning, this method lays a solid foundation for future work in cooperative multi-AUV systems, adaptive path planning, and decision-making under deep uncertainty. As autonomous systems become more common in defense applications, having simple and reliable tools to assess mission feasibility is not just helpful—it's critical.

References

[1] L. Zhang, D. Jiang, J. Zhao, and S. Ma, "An AUV for Ocean Exploring and its Motion Control System Architecture," The Open Mechanical Engineering Journal, vol. 7, no. 1, pp. 40–47, Oct. 2013, doi: https://doi.org/10.2174/1874155x01307010040.

[2] A. Vasilijevic, D. Nad, F. Mandic, N. Miskovic, and Z. Vukic, "Coordinated Navigation of Surface and Underwater Marine Robotic Vehicles for Ocean Sampling and Environmental Monitoring," IEEE/ASME Transactions on Mechatronics, vol. 22, no. 3, pp. 1174–1184, Jun. 2017, doi: https://doi.org/10.1109/tmech.2017.2684423.

[3] M. Faria et al., "Coordinating UAVs and AUVs for oceanographic field experiments: Challenges and lessons learned," 2014 IEEE International Conference on Robotics and Automation (ICRA), May 2014, doi: https://doi.org/10.1109/icra.2014.6907834.

[4] R. Martins, B. de, C. Carvalho Afonso, and M. L. Incze, "REP10 AUV: Shallow water operations with heterogeneous autonomous vehicles," Jun. 2011, doi: https://doi.org/10.1109/oceans-spain.2011.6003568.

[5] C. Mai, S. Pedersen, Leif Gjesing Hansen, Kasper Lund Jepsen, and Z. Yang, "Subsea infrastructure inspection: A review study," 2016 IEEE International Conference on Underwater System Technology: Theory and Applications (USYS), Dec. 2016, doi: https://doi.org/10.1109/usys.2016.7893928.

[6] P. Drews Jr, S. Botelho, and S. Gomes, "SLAM in Underwater Environment Using SIFT and Topologic Maps," pp. 91–96, Oct. 2008, doi: https://doi.org/10.1109/lars.2008.32.

[7] S. Azad, P. Casari, and M. Zorzi, "Coastal patrol and surveillance networks using AUVs and delay-tolerant networking," May 2012, doi: https://doi.org/10.1109/oceans-yeosu.2012.6263412.

[8] H. Kermorgant, "Architecture of AUV systems for harbour protection and mine countermeasure," Europe Oceans, pp. 1400–1405 Vol. 2, Jan. 2005, doi: https://doi.org/10.1109/oceanse.2005.1513266.

[9] L. Peruzzi, "Euronaval 2024 – SLAMF programme: the future of French Navy's mine warfare capabilities ," European Defense Review, Nov. 08, 2024. https://www.edrmagazine.eu/slamf-programme-the-future-of-french-navys-mine-warfare-capabilities (accessed Mar. 12, 2025).

[10] B. Szturomski, "The effect of an underwater explosion on a ship," Zeszyty Naukowe Akademii Marynarki Wojennej, vol. 201, no. 2, pp. 57–73, Jun. 2015, doi: https://doi.org/10.5604/0860889x.1172074.

[11] M. Larsen, "High performance Doppler-inertial navigation-experimental results," Nov. 2002, doi: https://doi.org/10.1109/oceans.2000.881808.

[12] L. Paull, S. Saeedi, M. Seto, and H. Li, "AUV Navigation and Localization: A Review," IEEE Journal of Oceanic Engineering, vol. 39, no. 1, pp. 131–149, Jan. 2014, doi: https://doi.org/10.1109/joe.2013.2278891.

[13] Luc Jaulin, Mobile Robotics. John Wiley & Sons, 2019.

[14] P. Corke, Robotics, Vision and Control. Springer Nature, 2023.

[15] S. Thrun, W. Burgard, and D. Fox, Probabilistic robotics. Cambridge, Mass.: Mit Press, 2010.

[16] Stephen Cole Kleene, Introduction to Metamathematics. 2012.

[17] N. Metropolis and S. Ulam, "The Monte Carlo Method," Journal of the American Statistical Association, vol. 44, no. 247, pp. 335–341, Sep. 1949, doi: https://doi.org/10.1080/01621459.1949.10483310.

[18] N. T. Thomopoulos, Essentials of Monte Carlo Simulation : Statistical Methods for Building Simulation Models. New York, Ny: Springer New York, 2013.

[19] A. Caiti, D. Martini, V. Morellato, and G. Vettori, "A Monte Carlo simulator for evaluation of AUV configuration in object search and classification missions," Europe Oceans 2005, pp. 1024–1027 Vol. 2, 2005, doi: https://doi.org/10.1109/oceanse.2005.1513198.

[20] R. E. Moore, R. Baker Kearfott, and M. J. Cloud, Introduction to Interval Analysis. SIAM, 2009.

[21] S. Rohou, Luc Jaulin, Lyudmila Mihaylova, F. L. Bars, and S. M. Veres, Reliable Robot Localization. John Wiley & Sons, 2019.

[22] IEEE Standard for Interval Arithmetic, IEEE 1788-2015, IEEE Computer Society, 2015.

[23] T. I. Fossen, Handbook of Marine Craft Hydrodynamics and Motion Control. John Wiley & Sons, 2021.

[24] M. F. Fathoni and A. I. Wuryandari, "Comparison between Euler, Heun, Runge-Kutta and Adams-Bashforth-Moulton integration methods in the particle dynamic simulation," 2015 4th International Conference on Interactive Digital Media (ICIDM), Dec. 2015, doi: https://doi.org/10.1109/idm.2015.7516314.